

## Use of cardiac radionuclide imaging to identify patients at risk for arrhythmic sudden cardiac death

Iosif Kelesidis, MD,<sup>a,b</sup> and Mark I. Travin, MD<sup>a,b</sup>

Sudden cardiac death (SCD) accounts for about 1/2 of all cardiovascular deaths, in most cases the result of a lethal ventricular arrhythmia. Patients considered at risk are often treated with an implantable cardiac defibrillator (ICD), but current criteria for device use, based largely on left ventricular ejection fraction (LVEF), leads to many patients receiving ICDs that they do not use, and many others not receiving ICDs but who suffer SCD. Thus, better methods of identifying patients at risk for SCD are needed, and radionuclide imaging offers much potential. Recent work has focused on imaging of cardiac autonomic innervation. <sup>123</sup>I-*m*IBG, a norepinephrine analog, is the tracer most studied, and a variety of positron emission tomographic tracers are also under investigation. Radionuclide autonomic imaging may identify at-risk patients with ischemic coronary artery disease, particularly following myocardial infarction and in the setting of hibernating myocardium. Most studies have been done in the setting of congestive heart failure (CHF), with a recent large multicenter study of patients with advanced disease, typically at high risk of SCD, showing that <sup>123</sup>I-*m*IBG can identify a low risk subgroup with an extremely low incidence of lethal ventricular arrhythmias and cardiac death, therefore, perhaps not requiring an ICD. Cardiac neuronal imaging has been shown to be better predictive of lethal arrhythmias/cardiac death than LVEF and New York Heart Association class, as well as various ECG parameters. Autonomic imaging will likely play an important role in the advancement of cardiac molecular imaging.

**Key Words:** Sudden cardiac death • cardiac autonomic imaging • <sup>123</sup>I-*m*IBG

### INTRODUCTION

Despite dramatic advances over the past five decades in the diagnosis and management of patients with cardiac disease, the incidence of sudden cardiac death (SCD) remains extraordinarily high, occurring in 184,000-462,000 people yearly, accounting for about 1/2 of all cardiovascular deaths.<sup>1</sup> SCD has been defined as “natural death from cardiac causes, heralded by abrupt loss of consciousness within 1 hour of onset of an acute change in cardiac status. Preexisting heart disease may

or may not have been known to be present, but the time and mode of death are unexpected.”<sup>2</sup> As the definition describes a sequence of events rather than a specific disease entity, and as its mechanism and causes are variable, and often unknown, effectively identifying patients at risk has been challenging, therefore limiting attempts at prevention. While high risk patients can often be identified, the majority who experience SCD had been considered to be low risk.<sup>3</sup>

In most cases (about 70%), and in a variety of clinical scenarios, the mechanism of SCD is a lethal ventricular tachyarrhythmia.<sup>4</sup> If a patient at risk can be identified, an implantable cardioverter defibrillator (ICD) can be implanted that can shock and/or pace the patient out of a lethal arrhythmia.<sup>5</sup> A left ventricular ejection fraction (LVEF) <30%-35% is the criterion currently used to identify patients at risk, and thus largely determines who gets an ICD as primary prevention. However, in a considerable number of patients who receive an ICD on this basis, the device never has to deliver therapy. At the same time, most patients who die suddenly have a higher LVEF and thus by current

From the Department of Nuclear Medicine,<sup>a</sup> Division of Cardiology/Department of Medicine,<sup>b</sup> Montefiore Medical Center, Albert Einstein College of Medicine, Bronx, NY.

Reprint requests: Mark I. Travin, MD, Department of Nuclear Medicine, Montefiore Medical Center, Albert Einstein College of Medicine, 111 East-210th Street, Bronx, NY 10467-2490; [mtravin@montefiore.org](mailto:mtravin@montefiore.org).

J Nucl Cardiol 2012;19:142-52.

1071-3581/\$34.00

Copyright © 2011 American Society of Nuclear Cardiology.

doi:10.1007/s12350-011-9482-9

guidelines do not qualify for ICD placement. Therefore, a parameter other than LVEF is needed to better select patients at risk for lethal ventricular arrhythmias who need an ICD, i.e., more effectively identify patients with low LVEF who will not benefit from an ICD, and find patients at risk for SCD but because of apparent (by LVEF) preserved cardiac function are not being considered for the device.<sup>6</sup>

Cardiac radionuclide imaging offers a variety of methods for identifying patients at risk for SCD from ventricular arrhythmias, therefore potentially offering a way to select patients for an ICD better than current methods. In this review, the potential utility of nuclear imaging, including standard perfusion tracer imaging but especially also the more promising use of autonomic radiotracers, to identify increased risk of lethal ventricular arrhythmias will be described. The focus will be on patients who already have symptoms or known cardiac problems, including in the settings of ischemic coronary artery disease (CAD), LV dysfunction associated with congestive heart failure (CHF) and cardiomyopathies, and primary cardiac arrhythmias.

### THE ROLE OF RADIONUCLIDE IMAGING IN PATIENTS WITH ISCHEMIC CAD

Most (about 80%) SCDs occur in the setting of ischemic heart disease, often in the setting of an acute coronary syndrome from plaque rupture.<sup>7</sup> Identification of extensive CAD can find patients at increased risk, and several studies by investigators at Duke have shown that severe and extensive defects on stress myocardial perfusion imaging (MPI) correlate with near- and long-term occurrence of SCD. In a study of 6,383 patients with known CAD who underwent stress <sup>99m</sup>Tc-sestamibi SPECT imaging, Piccini et al<sup>8</sup> found that a high summed stress score (SSS) was associated with SCD over a 6-year follow-up, independent of LVEF and the Charlson clinical co-morbidity index. A subsequent analysis of the data showed that the SSS also had an independent predictive value for supposedly lower risk patients who had an LVEF > 35%.<sup>9</sup>

Unfortunately, the value of stress perfusion imaging for prediction of SCD, i.e., the positive predictive value of an abnormal test, is low because the ability to identify specific patients who have coronary plaques at high risk of acute rupture is not now possible with MPI. In addition, patients with subclinical disease, which may include non-significant arterial narrowings not detected by perfusion imaging, are also at risk of acute plaque rupture and SCD. Several investigators have reported on the potential for imaging of unstable coronary plaques with <sup>18</sup>F-FDG (fluorodeoxyglucose) to identify active inflammation, often combined with CT imaging for

anatomic localization, but there remain technical and biological challenges to this method.<sup>10</sup>

Thus, radionuclide image identification of patients with known or subclinical CAD who are at risk for SCD from an acute coronary event such that specific interventions could be undertaken (other than standard risk factor reduction and conventional medical and invasive treatments) is not currently possible. As treatment of the underlying ischemia is the proper approach in these patients, an ICD would not play a major role in preventing SCD other than perhaps in those with extensive CAD and recurrent ischemia not amenable to revascularization.

### Post-Myocardial Infarction

Nevertheless, once ischemic damage has occurred, such from an acute myocardial infarction (MI), the situation has changed. The pathophysiology of the post-MI state is complex and dynamic, and offers more possibilities for radionuclide and other forms of imaging to identify patients at risk. As an infarct heals over days, weeks, and months, changes in tissue composition of the infarct area, the peri-infarct zone, and in remote regions may occur, all creating substrates for arrhythmias.<sup>11-13</sup> There may also be ongoing ischemia. Results of several trials—the Defibrillator in Acute Myocardial Infarction Trial (DINAMIT)<sup>14</sup> and the second Multicenter Automatic Defibrillator Implantation Trial (MADIT II)<sup>15</sup>—have indicated that while SCD is a significant problem, particularly in the first week post-MI, an ICD improves survival only after the first 40 days, with interestingly an increase in non-SCD in the early period in patients who receive an ICD.<sup>16,17</sup> In addition, clinical predictors of SCD, including the ability of LVEF to predict outcome, change over time.<sup>18</sup>

Thus, better methods are needed to identify post-MI patients at risk for lethal arrhythmias. Post-MI arrhythmias are related to a complex interplay of various factors, including abnormal anatomic substrate, depolarization heterogeneity, repolarization disruption, and autonomic dysfunction, with a lethal arrhythmia often triggered by an initiating event such as an electrolyte abnormality or catecholamine surge.<sup>19-21</sup> These factors have been studied with various non-invasive techniques, including cardiac magnetic resonance imaging (MRI), signal averaged ECG (SAECG), assessment of T wave alternans and QT-dispersion, but there has been minimal success using these methods risk stratify for SCD.

However, an area of active investigation in the post-MI setting is assessment of cardiac autonomic innervation which plays a major role in sustaining cardiovascular hemodynamic and electrophysiologic harmony. There is evidence that both global and regional sympathetic denervation (anatomic loss of sympathetic nerves) or

dysinnervation (sympathetic dysfunction or stunning) predispose patients to ventricular arrhythmias.<sup>22</sup> Among the various methods available to assess cardiac autonomic innervation, radionuclide imaging shows promise for assessing the risk of SCD.<sup>23-26</sup> The most studied autonomic tracer is iodine-123 *meta*iodobenzylguanidine (<sup>123</sup>I-*m*IBG), a sympathetic neurotransmitter norepinephrine (NE) analogue. Various positron emission tomographic (PET) tracer NE analogues, such as C-11 hydroxyephedrine (<sup>11</sup>C-HED), <sup>11</sup>C-epinephrine, and <sup>11</sup>C-phenylephrine, have also been studied, and an <sup>18</sup>F tracer is under investigation.<sup>27</sup>

Most published literature and current clinical applicability of autonomic radionuclide imaging is of the sympathetic system (mediated by NE), with studies of the parasympathetic system (mediated by acetylcholine) mostly in animals. NE is produced in presynaptic sympathetic nerve terminals by a biochemical sequence starting with tyrosine, then stored in presynaptic vesicles. In response to stimuli, the vesicles are released into the synaptic space with free NE binding to post-synaptic myocyte receptors producing the desired cardiac effect. To control the response, there is a transporter protein-mediated, sodium, energy, and temperature-dependent process, known as “uptake-1,” by which free NE is taken back up into presynaptic terminals for storage or catabolic disposal. Some NE is also taken up by non-neuronal postsynaptic cells (i.e., the “uptake-2” system).<sup>24,28-30</sup> Chemical modification of guanethidine, a false neurotransmitter analog of NE, produces *meta*iodobenzylguanidine (*m*IBG) that is also taken up by the presynaptic uptake-1 pathway. This compound can be labeled with radioactive iodine-123 (<sup>123</sup>I) but unlike NE is not catabolized by monoamine oxidase (MAO), allowing it to localize in pre-synaptic nerve endings to a high enough concentration for imaging with a standard gamma camera.<sup>31</sup>

Details of <sup>123</sup>I-*m*IBG imaging have been described in prior reviews.<sup>32</sup> Intravenous injection is performed at rest, with the appropriate dosage not yet definitively established. 3-5 mCi (111-185 MBq) were used in earlier studies, but more recently doses up to 10 mCi (370 MBq) have been injected to obtain better tomographic images.<sup>33,34</sup> Planar and single photon emission computed tomographic (SPECT) images are obtained approximately 15 minutes after tracer administration (early), and again 3-5 hours later (late). Most investigators feel that late images are best representative of sympathetic function.

Interpretation of cardiac <sup>123</sup>I-*m*IBG images currently includes review of planar images for global cardiac tracer uptake, cardiac tracer washout between early and delayed planar images, and regional uptake on tomographic images. The standard measure of global

cardiac <sup>123</sup>I-*m*IBG uptake is the heart mediastinal ratio (H/M), derived by assessment of per pixel activity in a region of interest over the heart in reference to background in the upper mediastinum.<sup>35</sup> A normal value used for H/M has been  $2.2 \pm 0.3$ , with values  $<1.6$  considered to be abnormal,<sup>31,34</sup> although normal values vary depending on the population studied (e.g., young vs older patients, differences in body habitus), and specific imaging techniques that may differ (e.g., variations in collimators used, methods of tracer labeling, etc). The H/M reflects receptor density and portrays both the integrity of presynaptic nerve terminals and uptake-1 function. A high ratio indicates predominant localization of the tracer in the myocardium that is expected for normal hearts, whereas a decreased ratio indicates less myocardial uptake and signifies reduced cardiac adrenergic receptor density. Examples of patients with normal and abnormal H/M ratios are shown in Figure 1.<sup>25</sup>

<sup>123</sup>I-*m*IBG washout may reflect turnover of catecholamines attributable to the sympathetic drive, and also reflects the ability of myocardium to retain tracer. A normal value has been reported to be 8.5%-10%.<sup>36</sup> Worsening heart failure is associated with a greater myocardial <sup>123</sup>I-*m*IBG washout rate (WR), often  $>27\%$ .<sup>37</sup>

Assessing regional uptake of <sup>123</sup>I-*m*IBG on tomographic images is less well established. The potential clinical utility of tomographic imaging is based on the concept that focal abnormalities may create electrical instability that predispose to dangerous ventricular arrhythmias, particularly if such territories are perfused and have viable myocytes, i.e., a neuronal/perfusion mismatch that creates denervation supersensitivity.<sup>38</sup>

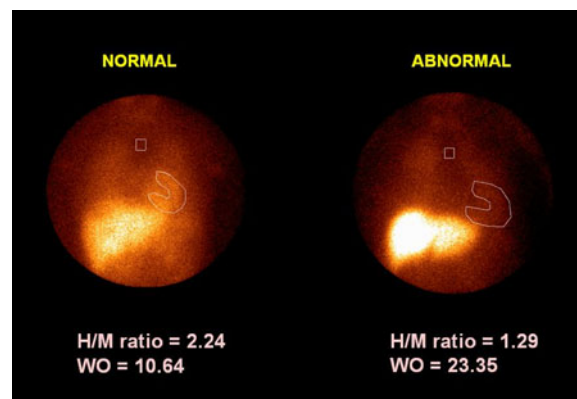


**Figure 1.** Examples of planar cardiac <sup>123</sup>I-*m*IBG images. The example on the left shows normal cardiac uptake with a H/M ratio of 2.24, and a normal tracer WR from initial to delayed images of 10.64% (not shown here). The example on the right shows an abnormal H/M ratio of 1.29 in images with an abnormal WR of 23.35%. H/M, Heart to mediastinal ratio; WR, washout rate (from Ji and Travin, with permission<sup>25</sup>).

However, the quality of  $^{123}\text{I}$ -*m*IBG tomographic images can be poor, particularly if there is extremely poor LV function, sometimes exacerbated by high liver and lung accumulation that interferes with cardiac visibility. In addition, methods of quantitative interpretation of tomograms are not established, in part because the relative uptake analysis approach used for perfusion imaging does not apply to  $^{123}\text{I}$ -*m*IBG images, and thus new methods need to be developed.

Various PET analogs of NE have also been studied. Besides having better physical properties for imaging, PET tracers are more similar to NE than  $^{123}\text{I}$ -*m*IBG.<sup>30</sup> The neuronal PET tracer most investigated is  $^{11}\text{C}$ -*meta*-hydroxyephedrine (HED), having higher uptake-1 selectivity than  $^{123}\text{I}$ -*m*IBG, allowing better differentiation of innervated from denervated myocardium, recently found to be particularly advantageous in evaluating hibernating myocardium.<sup>39</sup> In normal patients,  $^{11}\text{C}$ -HED has been shown to have more homogeneous uptake than  $^{123}\text{I}$ -*m*IBG, as does  $^{11}\text{C}$ -epinephrine.<sup>30,40</sup> Unfortunately, the short half life of  $^{11}\text{C}$  currently limits clinical applicability of  $^{11}\text{C}$  HED and similar compounds.

A tracer in the initial stages of investigation is LMI1195, designed similarly to  $^{123}\text{I}$ -*m*IBG but incorporating the longer lived  $^{18}\text{F}$  PET isotope, therefore more clinically practical. LMI1195 has a similar cellular uptake profile to NE, and comparable NET (norepinephrine transport)-binding affinity and NET-mediated cell uptake kinetics. In vivo studies demonstrate high cardiac uptake, producing high quality PET imaging. Imaging in rats with heart failure has shown that LMI1195 heart uptake levels decrease with disease progression. This promising tracer is expected to undergo intense investigation over the coming years.<sup>27</sup>

Among the earliest reports of potential benefit of autonomic imaging is in the post-MI setting, looking specifically for patients at risk for ventricular arrhythmias. Stanton et al<sup>41</sup> found that infarct  $^{123}\text{I}$ -*m*IBG defects are frequently larger than  $^{201}\text{Tl}$  defects, and that patients with mismatch ( $^{123}\text{I}$ -*m*IBG larger than  $^{201}\text{Tl}$ ) have more ventricular arrhythmias on Holter monitoring. McGhie et al<sup>42</sup> also showed that post-MI  $^{123}\text{I}$ -*m*IBG defects are more extensive than  $^{201}\text{Tl}$  defects and associated with increased ventricular arrhythmias.

Sympathetic innervation is more sensitive to oxygen deprivation than myocytes, with the area of injury more widespread (i.e., more apical) in the instance of transmural infarct (in part because the sympathetic nerve trunks traverse the area of injury), and neuronal dysfunction often persists longer than myocyte abnormalities.<sup>43</sup> In 12 dogs in which transmural infarcts were artificially created and imaged with  $^{123}\text{I}$ -*m*IBG, Dae et al<sup>44</sup> found that not only were there scar zones of absent  $^{123}\text{I}$ -*m*IBG and absent thallium uptake but also denervated (reduced  $^{123}\text{I}$ -*m*IBG

uptake) yet viable (preserved thallium uptake) zones distal to the infarct. Matsunari studied 12 patients following acute MI, and found that 1 week after infarction denervated regions by  $^{123}\text{I}$ -*m*IBG were significantly larger than final infarct sizes found by  $^{99\text{m}}\text{Tc}$ -sestamibi, with denervated areas instead being similar in size to the pre-infarct region at risk (i.e., regions subject to ischemia but not infarcted had residual autonomic injury despite return of perfusion tracer uptake).<sup>45</sup>

Work with dogs by Minardo et al showed that regions of sympathetic denervation by  $^{123}\text{I}$ -*m*IBG but with preserved perfusion by  $^{201}\text{Tl}$  have, using electrophysiological response techniques, supersensitive refractory period shortening that persist for as long as 3 weeks, i.e., areas of denervation supersensitivity. These regions are arrhythmogenic with an increased likelihood of ventricular fibrillation induction<sup>38,46,47</sup> Clinical evidence for this possibility was shown by Simões et al<sup>48</sup> in which 67 patients within 14 days of MI underwent rest imaging with  $^{123}\text{I}$ -*m*IBG and  $^{201}\text{Tl}$ . Consistent with the aforementioned work, the mean  $^{123}\text{I}$ -*m*IBG defect size was larger than the mean  $^{201}\text{Tl}$  defect size in 90% of patients, with a mismatch size of  $10 \pm 18\%$  (range = 0%-59%). ECG variables that have been associated with lethal ventricular arrhythmias—significant prolongation of the heart rate corrected QT interval (QTc) and evidence of delayed depolarization on SAECG—were associated with mismatch size, although there were too few lethal cardiac events in the short (0.7-year mean) follow-up to show a correlation with adverse outcome in this cohort of patients who generally had small infarcts and preserved LV function.

Sasano et al<sup>49</sup> created an infarct model in pigs, with artificial occlusion of the left anterior descending (LAD) artery. In a study of 11 such pigs, the mean autonomic innervation defect size measured by the PET tracer  $^{11}\text{C}$ -epinephrine was larger than the mean perfusion defect size imaged with  $^{11}\text{NH}_3$ , with an innervation/perfusion mismatch of  $7\% \pm 4\%$ . Pigs with larger mismatch sizes were significantly more likely to have inducible monomorphic ventricular tachycardia (VT), further supporting the contention that an infarct border zone of innervation/perfusion mismatch is an important contributor to post-MI lethal arrhythmias.

Bax et al<sup>50</sup> performed  $^{123}\text{I}$ -*m*IBG imaging on 50 patients with prior MI and LVEF < 40% who were referred for electrophysiological testing. Surprisingly, in these patients an innervation/perfusion mismatch was not associated with an inducible arrhythmia, or was the late H/M. However, the summed  $^{123}\text{I}$ -*m*IBG SPECT score that represents the size of global denervation was significantly higher in inducible than in non-inducible patients, with this variable being the only significant predictor by multivariable analysis, shown in Figure 2.

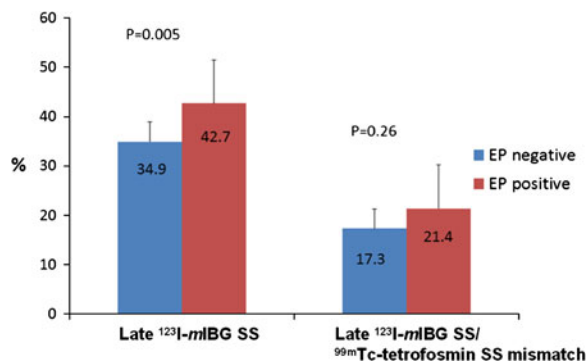


**Figure 2.** Relationship of EP inducible ventricular arrhythmias (i.e., “EP positive”) to <sup>123</sup>I-*m*IBG SPECT defects in patients with prior MI and LV dysfunction. The mean SS was significantly higher in patients who were EP positive than in those who were EP negative (*left* images), while there was no significant relationship of the mean <sup>123</sup>I-*m*IBG/<sup>99m</sup>Tc-tetrofosmin SS mismatch score to EP inducibility (*right* images). *EP*, Electrophysiologic; *SS*, summed score (data from Bax et al<sup>50</sup>).

As discussed, though, tomographic imaging with autonomic agents is still under investigation. More work is required to determine the role of autonomic imaging in the post-MI patient, possibly also with accompanying detailed anatomic investigation of the peri-infarct border zone using cardiac MRI, for determining who benefits from an ICD. Serial imaging may be crucial since the situation is dynamic.

### Autonomic Imaging of Hibernating Myocardium

CAD patients for whom autonomic imaging may be particularly useful are those with viable but chronically dysfunctional, i.e., “hibernating” myocardium. Observational studies suggest that this pathological substrate increases cardiac death, and abnormalities of sympathetic nerve function are likely contributory.<sup>51,52</sup> There may be a role for an ICD as primary prevention here. Using a porcine model, Canty, Fallavollita, Luisi and colleagues<sup>39,53,54</sup> have shown that creating a 1.5-mm LAD stenosis, producing a region of chronic hibernating myocardium, results in large regional <sup>11</sup>C-HED defects that increase in size and severity during the first 3 months, and persist for at least 2 months more. Previous work by this group had shown that pigs with hibernating myocardium are at increased risk of an arrhythmic SCD that is associated with sympathetic inhomogeneity.<sup>39,55</sup>

Similar abnormalities of sympathetic nerve function in chronic ischemic heart disease without infarction have been described in humans. Hartikainen et al reported <sup>123</sup>I-*m*IBG defects in almost all patients with significant stenosis (>50% diameter), with defect size

increasing as a function of stenosis severity. Among those with a severe stenosis (>90% diameter), <sup>123</sup>I-*m*IBG defect size was indistinguishable from patients with previous MI.<sup>52</sup> Bulow et al<sup>56</sup> reported similar findings using <sup>11</sup>C-HED.

An important question is which tracer is best in this setting. In pigs with hibernating myocardium, a 48% ± 3% regional reduction in <sup>11</sup>C-HED retention by PET imaging was found.<sup>53</sup> In contrast, the relative difference in <sup>123</sup>I-*m*IBG retention quantified with the more sensitive technique of ex vivo tissue counting was only 25% ± 3%.<sup>39</sup> Thus, PET imaging of <sup>11</sup>C-HED appears to provide an improved signal-to-noise ratio over <sup>123</sup>I-*m*IBG, with an almost twofold improvement in defect severity, and would likely facilitate quantitative regional analysis.

The potential of radionuclide sympathetic imaging to assess risk of SCD in the setting of hibernating myocardium is being investigated in the Prediction of Arrhythmic Events with PET (PAREPET) trial.<sup>57</sup> This observational cohort study has thus far enrolled >200 patients with ischemic cardiomyopathy (New York Heart Association (NYHA) functional Class I-III CHF, EF ≤ 35%) who are not under consideration for coronary revascularization. PET perfusion imaging uses <sup>13</sup>NH<sub>3</sub> (nitrogen-13 ammonia), viability imaging uses <sup>18</sup>FDG, and <sup>11</sup>C-HED imaging assesses sympathetic innervation. Preliminary data demonstrate that there is significant variability in the extent of viable, dysinnervated myocardium, from small borders around areas of infarction to large confluent regions encompassing several myocardial segments, shown in Figure 3.<sup>22</sup> PAREPET should help determine the clinical importance of the various image patterns by testing the hypothesis that the presence or volume (% of LV) of dysinnervated but viable myocardium can predict SCD (primary outcome) or cardiac mortality (secondary outcome), and serve as a guide to ICD therapy.

### THE ROLE OF AUTONOMIC IMAGING IN HEART FAILURE

Congestive heart failure is increasing throughout the world. As CHF largely involves disruption of the neurohormonal state, neuronal innervation plays a key role in the pathophysiology. An increased sympathetic response in patients with reduced cardiac output produces deleterious neurohormonal and myocardial structural changes that worsen the condition and increase the likelihood of arrhythmic SCD. Autonomic imaging provides independent prognostic information, and promises to help guide ICD use better than current approaches.

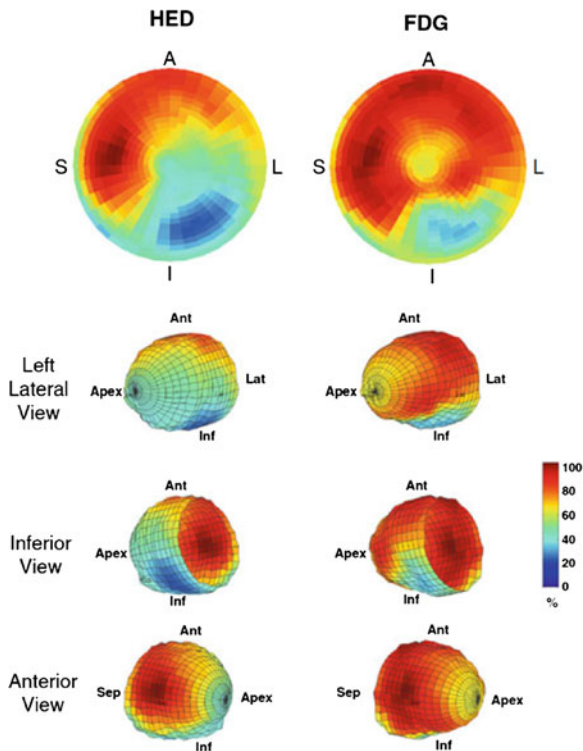


**Figure 3.** Example of a common autonomic (HED) and infarct (FDG) imaging pattern seen after myocardial infarction, from a subject in the PAREPET study. These PET polar tomograms and wire diagrams of the left ventricle illustrate relative tracer uptake, color coded from maximum activity in red to minimum activity in blue. The sympathetic nerve tracer  $^{11}\text{C}$ -meta-hydroxyephedrine (HED) defect (left images) involves a significantly larger myocardial area than the inferolateral scar seen by metabolic  $^{18}\text{F}$ -2-deoxyglucose (FDG) scanning (right images), indicating extensive viable but denervated myocardium. In addition to denervation at the periphery of the infarct, there is apical extension due to interruption of the sympathetic nerves that course across the heart from the base to the apex. Ant, Anterior wall; Sep, interventricular septum; LAT, lateral wall; Inf, inferior wall (from Fallavollita and Canty Jr, with permission<sup>22</sup>).

Studies have consistently shown that a decreased  $^{123}\text{I}$ -mIBG H/M predicts a poor prognosis in advanced CHF.<sup>58</sup> One of the first studies was by Merlet et al<sup>59</sup> in which patients with a mean LVEF of 22% and a H/M < 1.2 had a 12-month survival of 40% versus 100% for patients with higher ratios, with H/M superior to LVEF and heart size. Nakata et al<sup>60</sup> showed that prognosis progressively worsened as the H/M became lower, and his group also demonstrated that H/M predicted outcomes for both ischemic and non-ischemic CHF.<sup>61</sup>

Among the first multicenter studies was that by Agostini et al involving 6 European sites that followed 290 patients of >2 years. By logistic regression the only significant predictors of major events—cardiac death,

need for transplant, and potentially fatal arrhythmias—were LVEF and H/M.<sup>33</sup>

Subsequently, the international multicenter ADMIRE-HF (AdreView Myocardial Imaging for Risk Evaluation in Heart Failure, AdreView =  $^{123}\text{I}$ -mIBG) study, involving 961 patients in 96 US, Canadian, and European sites, was completed.<sup>34,62</sup> ADMIRE-HF reported that for patients with NYHA Class II-III CHF and LVEF  $\leq 35\%$ , a H/M < 1.6 on a 4-hour late  $^{123}\text{I}$ -mIBG image was more than doubled (from 15% to 37%) the 17-month incidence of worsening CHF, life-threatening arrhythmias, and cardiac death. Importantly, the predictive value held for all three event endpoints separately. In particular, there were only 2 deaths (<1%) of the 201 patients with H/M  $\geq 1.6$ , illustrated in Figure 4.<sup>26</sup> Subsequent multivariate analysis showed that H/M was a predictor of cardiac and all-cause deaths independent of other clinical and image variables, including age, LVEF, and BNP (brain natriuretic peptide).<sup>63</sup>

Interestingly, norepinephrine levels, although a univariate predictor of events in ADMIRE-HF, were not an independent multivariate predictor. The relationship between circulating norepinephrine levels and cardiac  $^{123}\text{I}$ -mIBG uptake is unclear, and at least one study showed no correlation.<sup>64</sup> Likely the relationship varies based on the stage of heart failure, perhaps with elevated levels of circulating NE in early stages competing with  $^{123}\text{I}$ -mIBG and leading to increased washout, but in later stages that are characterized by either loss of neurons or downregulation of presynaptic uptake, decreased tracer uptake is no longer affected by circulating NE.<sup>65</sup>

SCD from a ventricular arrhythmia is a major cause of death in patients with CHF, and in many cases strikes

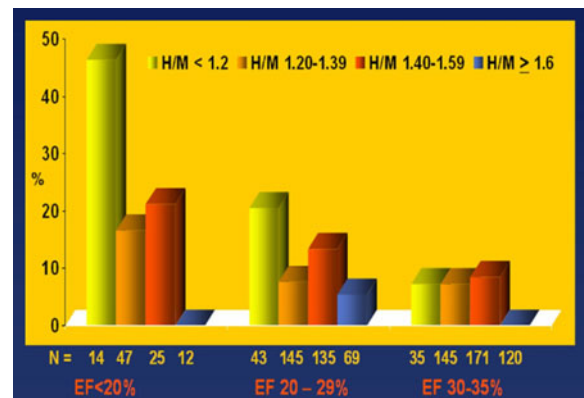


**Figure 4.** Relationship of EF and H/M groups to 2-year cardiac mortality (%). 201 patients (21% of total) had H/M > 1.6, with only 2 (<1%) cardiac deaths (one arrhythmic, one progressive heart failure). EF, Ejection fraction (left ventricular), H/M, heart mediastinal ratio (from Chirumamilla and Travin, with permission<sup>26</sup>).

patients who are otherwise relatively well.<sup>19</sup> Based on large clinical trials, i.e., Sudden Cardiac Death in Heart Failure Trial (SCD-HEFT), Comparison of Medical Therapy, Pacing, and Defibrillation in Heart Failure (COMPANION), and Defibrillators in Non-ischemic Cardiomyopathy Treatment Evaluation (DEFINITE), guidelines indicate that NYHA Class II-III CHF and LVEF  $\leq 35\%$  is a Class IA indication for ICD implantation as primary prevention.<sup>5,66-68</sup> Nevertheless, most patients who receive an ICD based on these criteria do not use their device,<sup>69</sup> with it widely acknowledged that LVEF is an imperfect predictor of arrhythmic death.<sup>6</sup> Appropriate ICD firings occur in only 5% of patients (per year),<sup>66</sup> and the number needed to treat to abort a life-threatening arrhythmia is about 20.<sup>69</sup> There are risks associated with an ICD, including a 4% post-procedural complication rate,<sup>70</sup> infection, device malfunction, worsened quality of life, psychiatric problems sometimes associated with shocks, and life style restrictions.<sup>71,72</sup> The cost is about \$28,000 per device.<sup>73</sup> Thus, a better approach for deciding who with advanced CHF should get an ICD is needed.<sup>74</sup>

While mechanisms of cardiac arrhythmias are complex and multifactorial, cardiac autonomic innervation is a crucial component,<sup>23</sup> suggesting a role for <sup>123</sup>I-*m*IBG imaging to better select patients for an ICD. As performing clinical studies on SCD is difficult, particularly given that ascertaining a definitive arrhythmic cause of death is often not possible, suitable patients to investigate are those who already have an ICD. Although occurrence of an ICD shock in these patients does not necessarily mean that they would have experienced SCD if not for the device,<sup>75,76</sup> it is currently an accepted method.

There are a few small studies evaluating the association of H/M with ICD discharges. Arora et al<sup>77</sup> performed a pilot study on 17 patients with advanced CHF and an ICD. A decreased late H/M (threshold 1.54) was associated with increased incidence of an ICD discharge. As in Figure 5, when autonomic imaging was combined with heart rate variability (HRV), a group of patients with no ICD discharges, and another group who all had discharges, were identified (although the very small patient number limits these findings). On tomographic imaging, patients who had ICD discharges had more extensive <sup>123</sup>I-*m*IBG/perfusion (<sup>99m</sup>Tc-sestamibi) mismatches, with case examples seen in Figure 6.

A subsequent larger study by Nagahara et al<sup>78</sup> prospectively followed 54 CHF patients with an ICD, finding that late H/M correlated significantly and independently with appropriate ICD discharges and SCD. Another study of 60 ICD implanted patients by Nishisato et al showed that a combination of H/M on <sup>123</sup>I-*m*IBG planar images and the summed perfusion

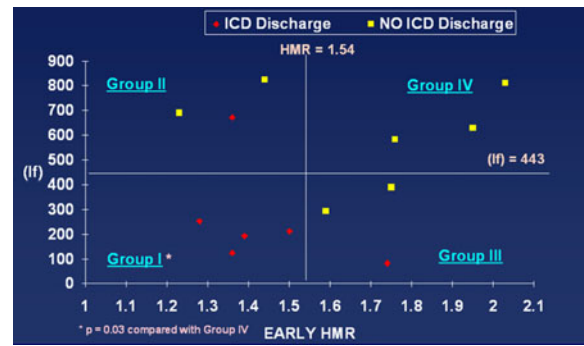


**Figure 5.** Relationship of a combination of <sup>123</sup>I-*m*IBG image results (HMR) and HRV variables (5-minute low frequency) to the occurrence of an ICD discharge. *HMR*, Heart mediastinal ratio; *HRV*, heart rate variability; *ICD*, implantable cardioverter defibrillator; *lf*, low frequency (modified from Arora et al, with permission<sup>77</sup>).

defect score (SS) on <sup>99m</sup>Tc-tetrafosmin SPECT images separated patients with device shocks from those without. Patients with an H/M  $\leq 1.9$  and SS  $\geq 12$  had a hazard ratio of 3.8 that by Cox regression analysis was independent and better than age, sex, SAECG, BNP, medications, inducible arrhythmias, and LVEF in predicting ICD shocks or cardiac death.<sup>79</sup>

High <sup>123</sup>I-*m*IBG WR has also been associated with increased risk. Kasama et al<sup>80</sup> showed an increased occurrence of SCD (hazard ratio = 1.15) with an increased WR. Tamaki et al compared ECG parameters—HRV, QT dispersion, and SAECG—with <sup>123</sup>I-*m*IBG findings in 106 patients with LVEF  $< 40\%$ ; those with SCD had a lower H/M and higher WR. By multivariate analysis only WR and LVEF were independent predictors of SCD, while ECG variables showed no relationship.<sup>81</sup> Interestingly abnormal WR also identified a group of patients with LVEF  $> 35$  at risk for SCD.

In ADMIRE-HF, combined “arrhythmic” events (i.e., self-limited VT, resuscitated cardiac arrest, appropriate ICD discharges) were more common in subjects with H/M  $< 1.60$  (10.4%) than in those with H/M  $\geq 1.6$  (3.5%  $P < .01$ ).<sup>62</sup> In a subanalysis of 578 patients without an ICD, Senior et al<sup>82</sup> reported only one fatal arrhythmic event in patients with H/M  $\geq 1.60$ , with the single event being in a patient with H/M = 1.6 (Figure 7).

<sup>123</sup>I-*m*IBG imaging with SPECT has also been reported helpful in recognizing arrhythmogenicity. Boogers et al demonstrated that over 3 years, a large <sup>123</sup>I-*m*IBG SPECT defect (summed score  $> 26$ ) predicted more frequent appropriate ICD therapy or cardiac death.<sup>83</sup>

Thus, studies consistently show that cardiac neuronal imaging is an independent predictor of adverse cardiac events, including arrhythmic events, and appear

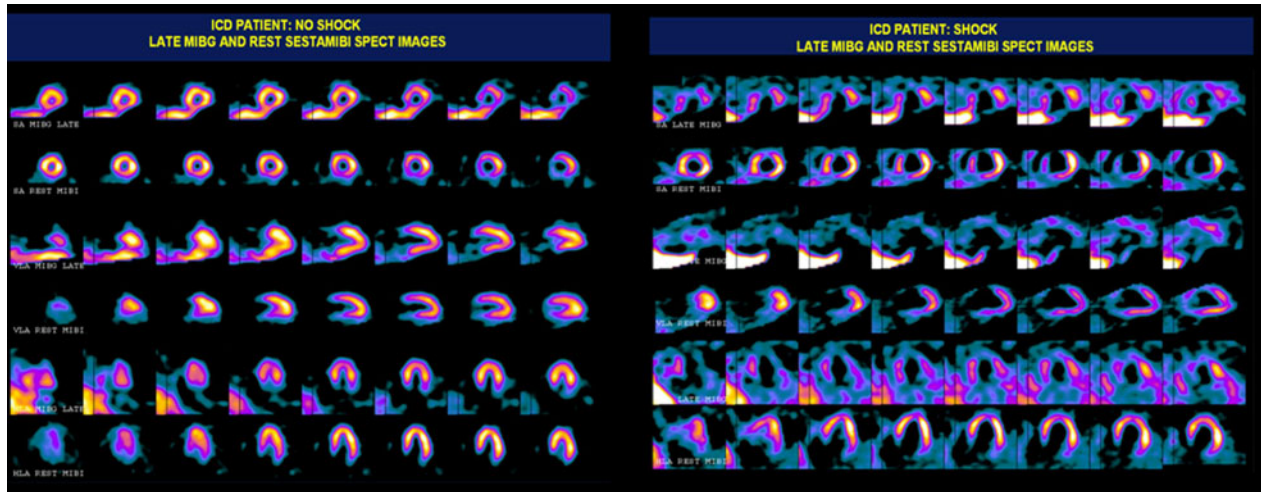


**Figure 6.**  $^{123}\text{I}$ -*m*IBG (neuronal) and  $^{99\text{m}}\text{Tc}$ -sestamibi (perfusion) SPECT images in patients with ICDs. The images on the *left* are from a patient without an ICD shock and show both homogeneous neuronal and perfusion tracer uptake. The images on the *right* are from a patient who had received numerous appropriate ICD shocks, and show neuronal/perfusion mismatching defects involving the inferior, inferolateral, and apical walls; there is a matched defect in the anterior wall. *HLA*, Horizontal long axis; *MIBG*, meta-iodobenzylguanidine ( $^{123}\text{I}$ -*m*IBG); *MIBI*,  $^{99\text{m}}\text{Tc}$ -sestamibi; *SA*, short axis (from Ji and Travin MI, with permission<sup>25</sup>).

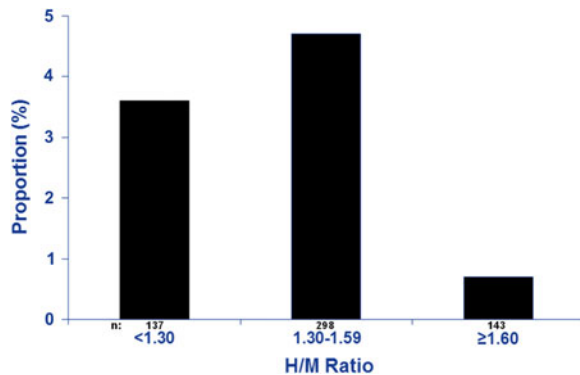


**Figure 7.** Occurrence of SCD ( $n = 20$ ) in the subset of ADMIRE-HF patients without an ICD ( $n = 578$ ). The lone subject in  $\text{H/M} \geq 1.6$  who had SCD had a ratio exactly at 1.6. *H/M*, Heart to mediastinal ratio; *ICD*, implantable cardioverter defibrillator (based on data from Senior et al<sup>82</sup>).

better than the currently accepted standards of LVEF and NYHA class. A satisfactory H/M has an extremely high negative predictive value for events. Larger, prospective studies are needed before there can be wider acceptance and inclusion of  $^{123}\text{I}$ -*m*IBG imaging in consensus guidelines, particularly since as discussed, prediction of an ICD shock does not necessarily indicate that the patient would have had SCD if not for the device.<sup>75,76</sup> At the same time, cardiac neuronal imaging could potentially identify patients in “lower risk” subgroups (e.g., LVEF > 35%) who are in fact at

significant risk of arrhythmic SCD and might benefit from an ICD.

### PRIMARY ARRHYTHMIAS

Neuronal tracer uptake abnormalities are seen in some primary arrhythmic disorders. In conditions such as idiopathic VT and arrhythmogenic right ventricular cardiomyopathy, PET and SPECT reveal altered neuronal function with no other structural abnormalities identified. Mitrani et al investigated  $^{123}\text{I}$ -*m*IBG imaging in patients presenting with VT in the absence of CAD. 67% of patients with VT had regional cardiac sympathetic denervation compared with 8% in control patients ( $P = .002$ ).<sup>84</sup> Gill et al<sup>85</sup> found asymmetrical uptake of  $^{123}\text{I}$ -*m*IBG in about half of the patients who had VT and “clinically normal” hearts, particularly obvious in patients with exercise-induced VT.

Neuronal tracer uptake abnormalities have been seen in more specifically characterized primary arrhythmic disorders. Schäfers et al<sup>86</sup> found abnormal  $^{11}\text{C}$ -HED distribution in patients with idiopathic right ventricular outflow tract tachycardia, as well as decreased uptake of the postsynaptic tracer  $^{11}\text{C}$ -CGP12177 (indicating reduced density of postsynaptic  $\beta$ -adrenoceptor density). In Brugada syndrome, that manifests as severe ventricular arrhythmias and sometimes SCD, neuronal tracer ( $^{11}\text{C}$ -HED) abnormalities appear localized to the inferior and inferoseptal walls.<sup>87</sup> Thus there may be a role of

cardiac imaging with neuronal radiotracers in guiding ICD therapy in primary arrhythmic disorders.

## CONCLUSIONS

Autonomic dysfunction plays a key role in the generation of life-threatening arrhythmias and SCD. There are a variety of roles for radionuclide imaging in identifying patients at risk who would benefit from an ICD. Neuronal radiotracers, such as  $^{123}\text{I}$ -*m*IBG, show potential for separating high from low risk patients, and appear to select patients who will benefit from ICD better than currently used techniques. In particular, global  $^{123}\text{I}$ -*m*IBG uptake above a certain level has a high negative predictive value for death and lethal arrhythmias; although, larger prospective studies are needed before this approach can be incorporated into guidelines and widely used. The development of PET neuronal tracers, and improved image analysis, promises to advance this powerful tool for effective guidance of therapy in patients at risk for SCD. Autonomic imaging will likely play an important role in the advancement of cardiac molecular imaging that visualizes key processes of cardiac pathophysiology.

## References

1. Goldberger JJ, Cain ME, Hohnloser SH, Kadish AH, Knight BP, Lauer MS, et al. American Heart Association /American College of Cardiology Foundation/Heart Rhythm Society scientific statement on noninvasive risk stratification techniques for identifying patients at risk for sudden cardiac death: A scientific statement from the American Heart Association Council on Clinical Cardiology Committee on Electrocardiography and Arrhythmias and Council on Epidemiology and Prevention. *J Am Coll Cardiol* 2008;52:1179-99.
2. Myerburg RJ, Castellanos RJ. Cardiac arrest and sudden cardiac death. In: Libby P, Bonow RO, Mann DL, Zipes DP, Braunwald E, editors. *Heart disease: A textbook of cardiovascular medicine*. 8th ed. Philadelphia: Saunders Elsevier; 2008. p. 733.
3. Exner DV, Klein GJ, Prystowsky EN. Primary prevention of sudden death with implantable defibrillator therapy in patients with cardiac disease. Can we afford to do it? (Can we afford not to?). *Circulation* 2001;104:1564-70.
4. Bayés de Luna A, Coumel P, Leclercq JF. Ambulatory sudden cardiac death: Mechanisms of production of fatal arrhythmia on the basis of data from 157 cases. *Am Heart J* 1989;117:151-9.
5. Jessup M, Abraham WT, Casey DE, Feldman AM, Francis GS, Ganiats TG, et al. Writing on behalf of the 2005 Guideline Update for the Diagnosis and Management of Chronic Heart Failure in the Adult Writing Committee. 2009 focused update: ACCF/AHA guidelines for the diagnosis and management of heart failure in adults: A report of the American College of Cardiology/American heart Association Task Force on Practice Guidelines. *J Am Coll Cardiol* 2009;53:1343-82.
6. Buxton AE, Lee KL, Hafley GE, Pires LA, Fisher JD, Gold MR, et al. Limitations of ejection fraction for prediction of sudden death risk in patients with coronary artery disease: Lessons from the MUSTT study. *J Am Coll Cardiol* 2007;50:1150-7.
7. Huikuri HV, Castellanos A, Myerburg RJ. Sudden death due to cardiac arrhythmias. *N Engl J Med* 2001;345:1473-82.
8. Piccini JP, Horton JR, Shaw LK, Al-Khatib SM, Lee KL, Iskandrian AE, et al. Single-photon emission computed tomography myocardial perfusion defects are associated with an increased risk of all-cause death, cardiovascular death, and sudden cardiac death. *Circ Cardiovasc Imaging* 2008;1:180-8.
9. Piccini JP, Starr AZ, Horton JR, Shaw LK, Lee KL, Al-Khatib SM, et al. Single-photon emission computed tomography myocardial perfusion imaging and the risk of sudden cardiac death in patients with coronary disease and left ventricular ejection fraction > 35%. *J Am Coll Cardiol* 2010;56:206-14.
10. Rudd JH, Narula J, Strauss HW, Virmani R, Machac J, Klimas M, et al. Imaging atherosclerotic plaque inflammation by fluorodeoxyglucose with positron emission tomography: Ready for prime time? *J Am Coll Cardiol* 2010;55:2527-35.
11. Chou CC, Zhou S, Hayashi H, Nihei M, Liu YB, Wen MS, et al. Remodelling of action potential and intracellular calcium cycling dynamics during subacute myocardial infarction promotes ventricular arrhythmias in langendorff-perfused rabbit hearts. *J Physiol* 2007;580:895-906.
12. Naud P, Guasch E, Nattel S. Physiological versus pathological cardiac electrical remodelling: Potential basis and relevance to clinical management. *J Physiol* 2010;588:4855-6.
13. Konstam MA, Kramer DG, Patel AR, Maron MS, Udelson J. Left ventricular remodeling in heart failure: Current concepts in clinical significance and assessment. *J Am Coll Cardiol Imaging* 2011;4:98-108.
14. Hohnloser SH, Kuck KH, Dorian P, Roberts RS, Hampton JR, Hatala R, et al. Prophylactic use of an implantable cardioverter-defibrillator after acute myocardial infarction. *N Engl J Med* 2004;351:2481-8.
15. Wilber DJ, Zareba W, Hall WJ, Brown MW, Lin AC, Andrews ML, et al. Time dependence of mortality risk and defibrillator benefit after myocardial infarction. *Circulation* 2004;109:1082-4.
16. Adabag AS, Therneau TM, Gersh BJ, Weston SA, Roger VL. Sudden death after myocardial infarction. *JAMA* 2008;300:2022-9.
17. Moss AJ, Vyas A, Greenberg H, Case RB, Zareba W, Hall WJ, et al. Temporal aspects of improved survival with the implanted defibrillator (MADIT-II). *Am J Cardiol* 2004;94:312-5.
18. Piccini JP, Zhang M, Pieper K, Solomon SD, Al-Khatib SM, Van de Werf F, et al. Predictors of sudden cardiac death change with time after myocardial infarction: Results from the VALIANT trial. *Eur Heart J* 2010;31:211-21.
19. Tomaselli GF, Zipes DP. What causes sudden death in heart failure? *Circ Res* 2004;95:754-63.
20. Zipes DP, Wellens HJ. Sudden cardiac death. *Circulation* 1998;98:2334-51.
21. Goldberger JJ, Passman R. Implantable cardioverter-defibrillator therapy after acute myocardial infarction. The results are not shocking. *J Am Coll Cardiol* 2009;54:2001-5.
22. Fallavollita JA, Canty JM Jr. Dysinnervated but viable myocardium in ischemic heart disease. *J Nucl Cardiol* 2010;17:1107-15.
23. Barron HV, Lesh MD. Autonomic nervous system and sudden cardiac death. *J Am Coll Cardiol* 1996;27:1053-60.
24. Verrier RL, Antzelevich C. Autonomic aspects of arrhythmogenesis: The enduring and the new. *Curr Opin Cardiol* 2003;19:2-11.
25. Ji SY, Travin MI. Radionuclide imaging of cardiac autonomic innervation. *J Nucl Cardiol* 2010;17:655-66.
26. Chirumamilla A, Travin MI. Cardiac applications of  $^{123}\text{I}$ -*m*IBG imaging. *Semin Nucl Med* 2011;41:374-87.

27. Yu M, Bozek J, Lamoy M, Guaraldi M, Silva P, Kagan M, et al. Evaluation of LMI1195, a novel 18F-labeled cardiac neuronal PET imaging agent, in cells and animal models. *Circ Cardiovasc Imaging* 2011;4:435-43.
28. Sisson JC, Wieland DM. Radiolabelled meta-iodobenzylguanidine pharmacology: Pharmacology and clinical studies. *Am J Physiol Imaging* 1986;1:96-103.
29. Flotats A, Carrio I. Cardiac neurotransmission SPECT imaging. *J Nucl Cardiol* 2004;11:587-602.
30. Bengel FM, Schwaiger M. Assessment of cardiac sympathetic neuronal function using PET imaging. *J Nucl Cardiol* 2004;11:603-16.
31. Hattori N, Schwaiger M. Metaiodobenzylguanidine scintigraphy of the heart: What have we learnt clinically? *Eur J Nucl Med* 2000;27:1-6.
32. Travin MI. Cardiac neuronal imaging at the edge of clinical application. *Cardiol Clin* 2009;27:311-27.
33. Agostini D, Verberne HJ, Burchert W, Knuuti J, Povince P, Sambuceti G, et al. I-123-mIBG myocardial imaging for assessment of risk for a major cardiac event in heart failure patients: Insights from a retrospective European multicenter study. *Eur J Nucl Med Mol Imaging* 2008;35:535-46.
34. Jacobson AF, Lombard J, Banerjee G, Camici PG. <sup>123</sup>I-mIBG scintigraphy to predict risk for adverse cardiac outcomes in heart failure patients: Design of two prospective multicenter international trials ADMIRE-HF study. *J Nucl Cardiol* 2009;16:113-21.
35. Flotats A, Carrió I, Agostini D, et al. Proposal for standardization of 123I-metaiodobenzylguanidine (MIBG) cardiac sympathetic imaging by the EANM Cardiovascular Committee and the European Council of Nuclear Cardiology. *Eur J Nucl Med Mol Imaging* 2010;37:1802-12.
36. Morozumi T, Kusuoka H, Fukuchi K, Tani A, Uehara T, Matsuda S, et al. Myocardial iodine-123-metaiodobenzylguanidine images and autonomic nerve activity in normal subjects. *J Nucl Med* 1997;38:49-52.
37. Ogita H, Shimonagata T, Fukunami M, et al. Prognostic significance of cardiac <sup>123</sup>I metaiodobenzylguanidine imaging for mortality and morbidity in patients with chronic heart failure: A prospective study. *Heart* 2001;86:656-60.
38. Minardo JD, Tuli MM, Mock BH, Weiner RE, Pride HP, Wellmann HN, et al. Scintigraphic and electrophysiologic evidence of canine myocardial sympathetic denervation and reinnervation produced by myocardial infarction or phenol application. *Circulation* 1988;78:1008-19.
39. Luisi AJ Jr, Fallavollita JA, Suzuki G, Cauty JM Jr. Spatial inhomogeneity of sympathetic nerve function in hibernating myocardium. *Circulation* 2002;106:779-81.
40. Lautamäki R, Tjipre D, Bengel FM. Cardiac sympathetic neuronal imaging using PET. *Eur J Nucl Med Mol Imaging* 2007;34:S74-85.
41. Stanton MS, Tuli MM, Radtke NL, Heger JJ, Miles WM, Mock BH, et al. Regional sympathetic denervation after myocardial infarction in humans detected noninvasively using I-123-Metaiodobenzylguanidine. *J Am Coll Cardiol* 1989;14:1519-26.
42. McGhie AI, Corbett JR, Akers MS, Kulkarni P, Sills MN, Kremers M, et al. Regional cardiac adrenergic function using I-123 Metaiodobenzylguanidine tomographic imaging after acute myocardial infarction. *Am J Cardiol* 1991;67:236-42.
43. Henneman MM, Bengel FM, Bax JJ. Will innervation imaging predict ventricular arrhythmias in ischaemic cardiomyopathy? *Eur J Nucl Med Mol Imaging* 2006;33:862-5.
44. Dae MW, Herre JM, O'Connell JW, Botvinick EH, Newman D, Munoz L. Scintigraphic assessment of sympathetic innervation after transmural versus nontransmural myocardial infarction. *J Am Coll Cardiol* 1991;17:1416-23.
45. Matsunari I, Schricke U, Bengel FM, Haase HU, Barthel P, Schmidt G, et al. Extent of cardiac sympathetic neuronal damage is determined by the area of ischemia in patients with acute coronary syndromes. *Circulation* 2000;101:2579-85.
46. Inoue H, Zipes DP. Results of sympathetic denervation in the canine heart: Supersensitivity that may be arrhythmogenic. *Circulation* 1987;75:877-87.
47. Kammerling JJ, Green FJ, Watanabe AM, Inoue H, Barber MJ, Henry DP, et al. Denervation supersensitivity of refractoriness in noninfarcted areas apical to transmural myocardial infarction. *Circulation* 1987;76:383-93.
48. Simões MV, Barthel P, Matsunari I, Nekolla SG, Schomig A, Schwaiger M, et al. Presence of sympathetically denervated but viable myocardium and its electrophysiologic correlates after early revascularised, acute myocardial infarction. *Eur Heart J* 2004;25:551-7.
49. Sasano T, Abraham MR, Chang KC, Ashikaga H, Mills KJ, Holt DP, et al. Abnormal sympathetic innervation of viable myocardium and the substrate of ventricular tachycardia after myocardial infarction. *J Am Coll Cardiol* 2008;51:2266-75.
50. Bax JJ, Kraft O, Buxton AE, Fjeld JG, Parizek P, Agostini D, et al. 123 I-MIBG scintigraphy to predict inducibility of ventricular arrhythmias on cardiac electrophysiology testing: A prospective multicenter pilot study. *Circ Cardiovasc Imaging* 2008;1:131-40.
51. Allman KC, Shaw LJ, Hachamovitch R, Udelson JE. Myocardial viability testing and impact of revascularization on prognosis in patients with coronary artery disease and left ventricular dysfunction: A meta-analysis. *J Am Coll Cardiol* 2002;39:1151-8.
52. Hartikainen J, Mustonen J, Kuikka J, Vanninen E, Kettunen R. Cardiac sympathetic denervation in patients with coronary artery disease without previous myocardial infarction. *Am J Cardiol* 1997;80:273-7.
53. Luisi AJ Jr, Suzuki G, Dekemp R, Haka MS, Toorongian SA, Cauty JM Jr, et al. Regional 11C-Hydroxyephedrine retention in hibernating myocardium: Chronic inhomogeneity of sympathetic innervation in the absence of infarction. *J Nucl Med* 2005;46:1368-74.
54. Fallavollita JA, Cauty JM Jr. Differential 18F-2-Deoxyglucose uptake in viable dysfunctional myocardium with normal resting perfusion: Evidence for chronic stunning in pigs. *Circulation* 1999;99:2798-805.
55. Cauty JM Jr, Suzuki G, Banas MD, Verheyen F, Borgers M, Fallavollita JA. Hibernating myocardium: Chronically adapted to ischemia but vulnerable to sudden death. *Circ Res* 2004;94:1142-9.
56. Bulow HP, Stahl F, Lauer B, Nekolla SG, Schuler G, Schwaiger M, et al. Alterations of myocardial presynaptic sympathetic innervation in patients with multi-vessel coronary artery disease but without history of myocardial infarction. *Nucl Med Commun* 2003;24:233-9.
57. Fallavollita JA, Luisi AJ Jr, Michalek SM, Valverde AM, deKemp RA, Haka MS, et al. Prediction of arrhythmic events with positron emission tomography: PAREPET study design and methods. *Contemp Clin Trials* 2006;27:374-88.
58. Verberne HJ, Brewster LM, Somsen GA, van Eck-Smit BL. Prognostic value of myocardial 123I-Metaiodobenzylguanidine (MIBG) parameters in patients with heart failure: A systematic Review. *Eur Heart J* 2008;29:1147-59.
59. Merlet P, Valette H, Dubois-Randé J, Moysé D, Duboc D, Dove P, et al. Prognostic value of cardiac metaiodobenzylguanidine in patients with heart failure. *J Nucl Med* 1992;33:471-7.

60. Nakata T, Miyamoto K, Doi A, Sasao H, Wakabayashi T, Kobayashi H, et al. Cardiac death prediction and impaired cardiac sympathetic innervation assessed by MIBG in patients with failing and nonfailing hearts. *J Nucl Cardiol* 1998;5:579-90.
61. Wakabayashi T, Nakata T, Hashimoto A, Yuda S, Tsuchihashi K, Travin MI, et al. Assessment of underlying etiology and cardiac sympathetic innervation to identify patients at high risk of cardiac death. *J Nucl Med* 2001;42:1757-67.
62. Jacobson AF, Senior R, Cerqueira MD, Wong ND, Thomas GS, Lopez VA, et al. Myocardial iodine-123 Meta-Iodobenzylguanidine imaging and cardiac events in heart failure. Results of the prospective ADMIRE-HF (AdreView Myocardial Imaging for Risk Evaluation in Heart Failure) study. *J Am Coll Cardiol* 2010;55:2212-21.
63. Travin M, Ananthasubramaniam K, Henzlova MJ, et al. Imaging of myocardial sympathetic innervation for prediction of cardiac and all-cause mortality in heart failure patients: Analyses from the ADMIRE-HF Trial. *Circulation* 2009;120:S350 (abstract).
64. Schofer J, Spielmann R, Schuchert A, Weber K, Schlüter M. Iodine-123 meta-iodobenzylguanidine scintigraphy: A noninvasive method to demonstrate myocardial adrenergic nervous system disintegrity in patients with idiopathic dilated cardiomyopathy. *J Am Coll Cardiol* 1988;12:1252-8.
65. Chen GP, Tablblazar R, Branch KR, Link JM, Caldwell JH. Cardiac receptor physiology and imaging: An update. *J Nucl Cardiol* 2005;12:714-30.
66. Bardy GH, Lee KL, Mark DB, et al. Amiodarone or an implantable defibrillator for congestive heart failure. *N Engl J Med* 2005;352:225-37.
67. Bristow MR, Saxon LA, Boehmer J, Krueger S, Kass DA, De Marco T, et al. Cardiac-resynchronization therapy with or without an implantable defibrillator in advanced chronic heart failure. *N Engl J Med* 2004;350:2140-50.
68. Kadish A, Dyer A, Daubert JP, Quiga R, Estes M, Anderson KP, et al. Prophylactic defibrillator implantation in patients with non-ischemic dilated cardiomyopathy. *N Engl J Med* 2004;350:2151-8.
69. Fisher JD, Ector HE. Relative and absolute benefits: Main results should be reported in absolute terms. *Pacing Clin Electrophysiol* 2007;30:935-7.
70. Lee DS, Krahn AD, Healey JS, Birnie D, Crystal E, Dorian P, et al. Evaluation of early complications related to de novo cardioverter defibrillator implantation insights from the Ontario ICD database. *J Am Coll Cardiol* 2010;55:774-82.
71. Anderson KP. Estimates of implantable cardioverter-defibrillator complications Caveat emptor. *Circulation* 2009;119:1069-71.
72. Anderson KP. Risk assessment for defibrillator therapy. *J Am Coll Cardiol* 2007;50:1158-60.
73. Sanders GD, Hlatky MA, Owens DK. Cost-effectiveness of implantable cardioverter-defibrillators. *N Engl J Med* 2005;353:1471-80.
74. Kadish A, Goldberger J. Selecting patients for ICD implantation: Are clinicians choosing appropriately? *JAMA* 2011;305:91-2.
75. Kim SG, Fisher JD, Furman S. Hypothetical death rates of patients with implantable defibrillators remain very hypothetical. *Am J Cardiol* 1993;72:1453-5.
76. Ellenbogen KA, Levine JH, Berger RD, Daubert JP, Winters SL, Greenstein E, et al. Are implantable cardioverter defibrillator shocks a surrogate for sudden cardiac death in patients with nonischemic cardiomyopathy. *Circulation* 2006;113:776-82.
77. Arora R, Ferrick KJ, Nakata T, Kaplan RC, Rozengarten M, Latif F, et al. I-123 MIBG imaging and heart rate variability analysis to predict the need for an implantable cardioverter defibrillator. *J Nucl Cardiol* 2003;10:121-31.
78. Nagahara D, Nakata T, Hashimoto A, Wakabayashi T, Kyuma M, Noda R, et al. Predicting the need for an implantable cardioverter defibrillator using cardiac metaiodobenzylguanidine activity together with plasma natriuretic peptide concentration or left ventricular function. *J Nucl Med* 2008;49:225-33.
79. Nishisato K, Hashimoto A, Nakata T, Doi T, Yamamoto H, Nagahara D, et al. Impaired cardiac sympathetic innervation and myocardial perfusion are related to lethal arrhythmia: Quantification of cardiac tracers in patients with ICDs. *J Nucl Med* 2010;51:1241-9.
80. Kasama S, Toyama T, Sumino H, Nakazawa M, Matsumoto N, Sato Y, et al. Prognostic value of serial cardiac <sup>123</sup>I-MIBG imaging in patients with stabilized chronic heart failure and reduced left ventricular ejection fraction. *J Nucl Med* 2008;49:907-14.
81. Tamaki S, Yamada T, Okuyama Y, Morita T, Sanada S, Tsukamoto Y, et al. Cardiac iodine-123 Metaiodobenzylguanidine imaging predicts sudden cardiac death independently of left ventricular ejection fraction in patients with chronic heart failure and left ventricular systolic dysfunction: Results from a comparative study with signal-averaged electrocardiogram, heart rate variability, and QT dispersion. *J Am Coll Cardiol* 2009;53:426-35.
82. Senior R, Agostini D, Travin M, et al. Imaging of myocardial sympathetic innervation for prediction of arrhythmic events in heart failure patients: Insights from the ADMIRE-HF trial. *Circulation* 2009;120:S349 (abstract).
83. Boogers MJ, Borleffs CJ, Henneman MM, van Bommel RJ, van Ramshorst J, Boersma E, et al. Cardiac sympathetic denervation assessed with 123-Iodine metaiodobenzylguanidine imaging predicts ventricular arrhythmias in implantable cardioverter-defibrillator patients. *J Am Coll Cardiol* 2010;55:2769-77.
84. Mitrani RD, Klein LS, Miles WM, Hackett FK, Burt RW, Wellman HN, et al. Regional cardiac sympathetic denervation in patients with ventricular tachycardia in the absence of coronary artery disease. *J Am Coll Cardiol* 1993;22:1344-53.
85. Gill JS, Hunter GJ, Gane J, Ward DE, Camm AJ. Asymmetry of cardiac [123I] Meta-iodobenzyl-guanidine scans in patients with ventricular tachycardia and a "Clinically Normal" heart. *Br Heart J* 1993;69:6-13.
86. Schäfers M, Lerch H, Wichter T, Rhodes CG, Lammertsma AA, Borggrefe M, et al. Cardiac sympathetic innervation in patients with idiopathic right ventricular outflow tract tachycardia. *J Am Coll Cardiol* 1198;32:181-6.
87. Wichter T, Matheja P, Eckardt L, Kies P, Schäfers K, Schulze-Bahr E, et al. Cardiac autonomic dysfunction in Brugada syndrome. *Circulation* 2002;105:702-6.